Remote pulsed laser Raman spectroscopy system for detecting water, ice, and hydrous minerals

Christopher S. Garcia[a], M. Nurul Abedin[b], Shiv K. Sharma[c], Anupam K. Misra[c], Syed Ismail[b], Upendra Singh[b], Tamer F. Refaat[a], Hani Elsayed-Ali[a], and Steve Sandford[b]
[a]Old Dominion University, Norfolk, VA 23529
[b]NASA Langley Research Center, Hampton, VA 23681
[c]University of Hawaii, Hawaii Inst. of Geophysics. & Planetology, Honolulu, HI-96822

ABSTRACT

For exploration of planetary surfaces, detection of water and ice is of great interest in supporting existence of life on other planets. Therefore, a remote Raman spectroscopy system was demonstrated at NASA Langley Research Center in collaboration with University of Hawaii for detecting ice-water and hydrous minerals on planetary surfaces. In this study, a 532 nm pulsed laser is utilized as an excitation source to allow detection in high background radiation conditions. The Raman scattered signal is collected by a 4-inch telescope positioned in front of a spectrograph. The Raman spectrum is analyzed using a spectrograph equipped with a holographic super notch filter to eliminate Rayleigh scattering, and a holographic transmission grating that simultaneously disperses two spectral tracks onto the detector for higher spectral range. To view the spectrum, the spectrograph is coupled to an intensified charge-coupled device (ICCD), which allows detection of very weak Stokes line. The ICCD is operated in gated mode to further suppress effects from background radiation and long-lived fluorescence. The sample is placed at 5.6 m from the telescope, and the laser is mounted on the telescope in a coaxial geometry to achieve maximum performance. The system was calibrated using the spectral lines of a Neon lamp source. To evaluate the system, Raman standard samples such as calcite, naphthalene, acetone, and isopropyl alcohol were analyzed. The Raman evaluation technique was used to analyze water, ice and other hydrous minerals and results from these species are presented.

Keywords: Raman Spectroscopy, pulsed laser, ICCD, isopropanol, acetone, naphthalene, calcite, hydrous minerals, water, ice.

1. INTRODUCTION

It has been proposed that Raman spectroscopy is a well suited tool for analyzing minerals and organic materials on planetary surface to detect traces of extinct and extant life.[1,2] Furthermore, detection of water on planetary and lunar surfaces is vital in supporting the existence of life on other planets.[3] Therefore, a remote Raman spectroscopy system was demonstrated for detecting water and ice-water on planetary surfaces. In addition, water molecules, if chemically bonded to other molecules, can exist in environments with temperature higher than the boiling point of water.[4] Therefore, by detecting chemically bonded water, presence of water can be found in dry environments which would otherwise show no sign of liquid water.

Raman spectroscopy is a powerful technique for determining the composition and the structure of a solid, liquid, or gas material based on its vibrational spectra.[5-7] Monochromatic light of known wavelength excites the molecules in the sample from a relaxed vibrational energy level into an excited virtual vibrational level. While most of the excited molecules return to the original vibrational level, releasing photons of the same wavelength as the excitation light (Rayleigh scattering), a few molecules return to a vibrational level that is higher than the relaxed level, causing photons with lower energy to be released (Stokes scattering). In some cases, the molecules begin from an excited vibrational level, then excited to a higher virtual level by the excitation source, and finally return to the relaxed vibrational level, releasing photons with higher energy (Anti-stokes scattering). Stokes and Anti-stokes scattering, although extremely weak compared to the Rayleigh scattering, provide compositional and structural information on the molecules present in the sample. In this study, we are interested in measuring the Stokes scattering as it is relatively stronger than Anti-Stokes scattering.

2. EXPERIMENTAL SETUP

Raman spectroscopy systems typically consist of four major sections, namely an excitation source, a light collection system, a spectrograph, and a detector. The excitation source is a monochromatic light of known wavelength, which is scattered by the molecules in the sample. All The scattered photons are collected by a light collection system (telescope). This optical system should be able perform two tasks: it should be able to collect the maximum amount of scattered light, and at the same time block the strong Rayleigh-scattered light. The collected light is then passed through a spectrograph, via optical fiber coupling or direct coupling. The spectrograph disperses the input light into its spectral components using a diffraction grating. The spectrograph output is detected by an array of photodetectors. The location of the spectral lines on the detector forms the Raman spectra.

The schematic diagram of the pulsed remote Raman spectroscopy system is shown in Figure 1 and described in detail below.

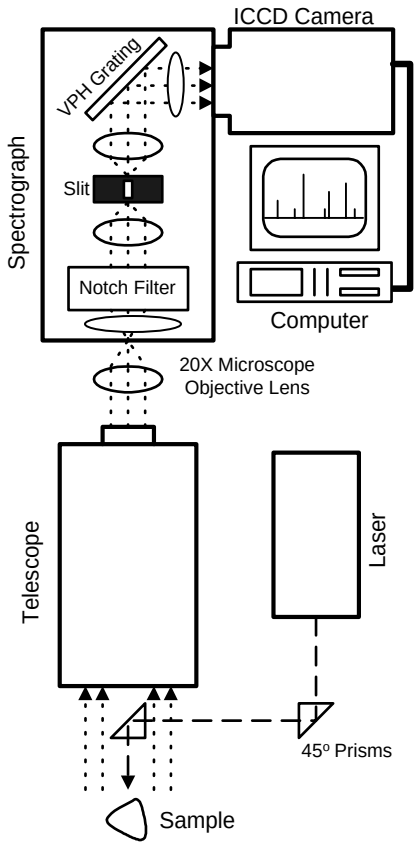

Figure 1. Schematic diagram of the remote pulsed laser Raman spectroscopy system.

2.1. Excitation Source

The excitation source was a mini Nd:YAG pulsed laser from Big Sky Laser (model UltraCFR) with a 532 nm wavelength, 45 mJ/pulse total energy, up to 20 Hz lasing frequency, and 8 ns pulse width. Using two 45°, 10 mm prisms, the laser beam is made collinear with the telescope's optical axis. This configuration, referred to as a coaxial geometry, permits scattered signal to be gathered from the target for the 180° back scattering to achieve maximum performance. The laser beam strikes the sample, which was placed about 5.6 m away.

2.2. Light Collection System

The remote scattered light was collected using a telescope (Meade ETX-105, Maksutov-Cassegrain Telescope) with a 4-inch aperture). Because fiber coupling results in significant signal attenuation, the telescope and output was directly attached to the spectrograph. A 20x microscope objective was placed between the telescope and the spectrograph to focus the telescope image into the spectrograph entrance aperture.

2.3. Spectrograph

Within the spectrograph (Kaiser Optical Systems, Inc. HoloSpec f/1.8i) the signal passed through a notch filter (Kaiser Optical 532 nm Holographic SuperNotch-Plus Filter) to remove the strong Rayleigh-scattered photons. As previously mentioned, this section of the system should be able to block the Rayleigh-scattered light. For this system, however, this filtering component was integrated in the spectrograph. The holographic notch filter allows a strong attenuation of the Rayleigh signal, while permitting a good transmission of the signal outside the rejection band.[8] The notch filter also features a very narrow rejection bandwidth, and sharp spectral edges. The transmitted signal was then focused through a 100 µm slit to define the resolution of the spectral lines, and finally passed through a holographic transmission grating (Kaiser Optical HoloPlex Transmission Grating) to disperse the signal into its spectral components. An important feature of the HoloPlex Transmission grating is that it simultaneously disperses two spectral tracks on the detector.[9] The low frequency portion of the spectra is dispersed on the upper half of the detector, whereas the high frequency portion is dispersed on the lower half. This ingenuous scheme doubles the range of the spectrograph, while maintaining the spectral resolution.

2.4. Detector

The spectra formed by the spectrograph was measured by a thermoelectrically cooled, gated, and intensified charge-coupled devices (ICCD) camera (Princeton Instruments PI-Max ICCD Camera) with 1024 x 256 pixels, and 26 µm x 26 µm pixel size. The ICCD detects extremely weak Stokes lines by adding a gain of up to 250 to the input signal.[10] This is implemented by first passing the input light signal through a photocathode that releases electrons from incident photons. The electrons are then accelerated through microchannel plates (MCP) i.e. Gen II, where they generate more electrons as they hit the channel walls. As the electron leave the MCP, they strike the phosphor coating on a fluorescent screen causing it to release photons which fall on the pixels of the CCD and generate charge. The horizontal position of the charge on the CCD defines the horizontal position of the spectral line, whereas the amount of charge generated defines its intensity. To display and analyze the resulting spectra, the CCD was connected to a computer, which contains the CCD application software (Princeton Instruments Winspec/32, Version 2.5F). The spectra were processed and analyzed using GRAMS/AI (Galactic Industries) software.

3. EXPERIMENTAL PROCEDURE

Several mineral samples were acquired from the University of Hawaii. Samples were placed ~5.6 meters from the system. Solid samples were characterized without any sample preparation, and placed on the sample stage, whereas liquid or granular samples were contained in glass vials. Calibration was first performed using a Neon lamp source (Oriel). The locations of the spectral lines of the Neon source in pixel number were compared to corresponding standard values in nanometers.

To collect the Raman spectrum for each sample, the laser was fired, and the camera was turned on for an integration time of 10 seconds. The “image” of the spectrum was recorded with the ICCD detector. The low and high frequency spectra of the sample were generated by getting the cross-section of the upper half and lower half region, respectively, of the recorded image. The horizontal axis of each resulting spectrum was converted into nanometers, then wave numbers, using the neon calibration data.

One of the features of this system was its ability to measure in high-background environment such as daylight and room lighting. This was achieved by gating the ICCD detector. The camera could be operated in a continuous mode, or gated

mode. In the continuous mode, the camera shutter was opened during a given integration time. This mode of operation is not practical for measurements under well-illuminated conditions because it allows background light signal such as mercury lines from room lights to be recorded on the spectra. In the gated mode, however, the CCD was turned on only for a very short time whenever the camera receives an external trigger signal. Since each laser pulse was only 8 ns long, and Raman-scattered photons were released instantaneously, the CCD was only turned on right before and right after each laser pulse, repeatedly during the 10 second integration time. To gate the camera to turn on the CCD, the "Lamp Sync" trigger from the flash lamp of the laser was used. The gate width, which is the duration that the CCD was turned on, was chosen to be 2 μs to cover the deviation in delay between the Lamp Sync trigger and the actual laser firing. Given that the pulse rate of the laser was 20 Hz, the CCD was only turned on for a mere total of 400 μs during the 10 second integration time. Therefore, the period during which background radiation is picked-up by the detector in gated mode is only 1/25,000 of that in the continuous mode.

To evaluate the performance of the Raman system, four standard samples (isopropanol, acetone, naphthalene, and calcite) were analyzed. The Raman spectra of ice, water, and other hydrous minerals ($FeSO_4 \cdot 7H_2O$, $MgSO_4 \cdot 7H_20$, $MgCl_4 \cdot 6H_2O$, and gypsum) were then measured.

4. RESULTS AND DISCUSSION

To evaluate the performance of the system, the Raman spectra of isopropanol, acetone, naphthalene and calcite were measured. The low frequency (0-2200 cm^{-1}) and high frequency (2200-4400 cm^{-1}) spectra are shown in Figures 2(a) and 2(b), respectively. For calcite the standard NIST values of its Raman fingerprints are 281.7 and 711 cm^{-1} and the symmetric stretching mode of carbonate is 1085 cm^{-1}. The peak positions measured by the Raman system at NASA Langley were 280, 711, and 1084 cm^{-1} within ±2 cm^{-1} of standard values obtained from the NIST website[11] for organic materials. The 10 second integration period was sufficient to generate high quality Raman spectra with highly defined peaks and bands. Furthermore, measurement under room-light illumination was successfully achieved as proven by the absence of mercury spectral lines in the low frequency Raman spectra.

The Raman spectra of ice and water were obtained and the high frequency regions are shown in Figure 3. The water sample was tap water in a glass beaker, and the ice sample was a cylindrical block with height and diameter of about 3 inches. In liquid water, strong broad Raman bands at 3270 and 3440 cm^{-1} were observed, and were due to symmetric and antisymmetric stretching O-H vibrational modes of water molecules, respectively. The strongest Raman bands are usually produced by the stretching vibrational modes. The Raman spectrum of ice shows a band around the same region as water, but it has a very strong and sharp band at 3140 cm^{-1}, making it easily distinguishable from liquid water. The decrease in the frequency od symmetric O-H stretching mode of water molecules in ice is due to formation of stronger hydrogen bond in ice that gives ice a more open (less dense) structure than liquid water.

Hydrous minerals, melanterite ($FeSO_4 \cdot 7H_2O$), epsomite ($MgSO_4 \cdot 7H_20$), bischofite ($MgCl_2 \cdot 6H_2O$), and gypsum ($CaSO_4 \cdot 2H_2O$), were analyzed and their high frequency Raman spectra are shown in Figure 4. The Raman spectrum of gypsum has very sharp and two strong bands 3400 and 3487 cm^{-1}, which are due to the stretching modes of water molecules, and indicate the presence of chemically bonded two types of water molecules in an ordered structure[12,13]. Water molecules can exist in these minerals at temperatures significantly above the boiling point of water because the water molecules are chemically bonded with the minerals. The Raman spectrum of $MgCl_2 \cdot 6H_2O$ has two well defined O-H stretching bands at 3350 and 3507 cm^{-1} (Fig. 4) indicating presence of at least two distict type of water molecules. Neutron diffraction study of $MgCl_2 \cdot 6H_2O$ has indicated that the monoclinic structure of this mineral can be considered to be composed of $Cl^-(H_2O)_3Mg^{2+}(H_2O)_3Cl^-$ groups with crystallographic point-group symmetry 2/**m**.[14]

In the Raman spectrum of $MgSO_4 \cdot 7H_20$ and $FeSO_4 \cdot 7H_2O$ broad overlapping O-H bands are observed in the O-H stretching region. These spectral features are the same as reported in a recent micro-Raman study.[15] Neutron diffraction studies of of some isostructural hepta- and tetrahydrates, including $CoSO_4 \cdot nD_2O$ (n = 4 and 7) and $MgSO_4 \cdot 4H_2O$.[16,17] These studies revealed seven and four different types of crystallographic distinct, asymmetric water molecules in $CoSO_4 \cdot 7D_2O$ and $CoSO_4 \cdot 4D_2O$, respectively, all occupied in C_1 sites. We believe these hydrates qualitatively reflect the structures of the X_2O molecules and H-bonding in the $FeSO_4 \cdot 7H_2O$ and $MgSO_4 \cdot 7H_20$ hydrates.

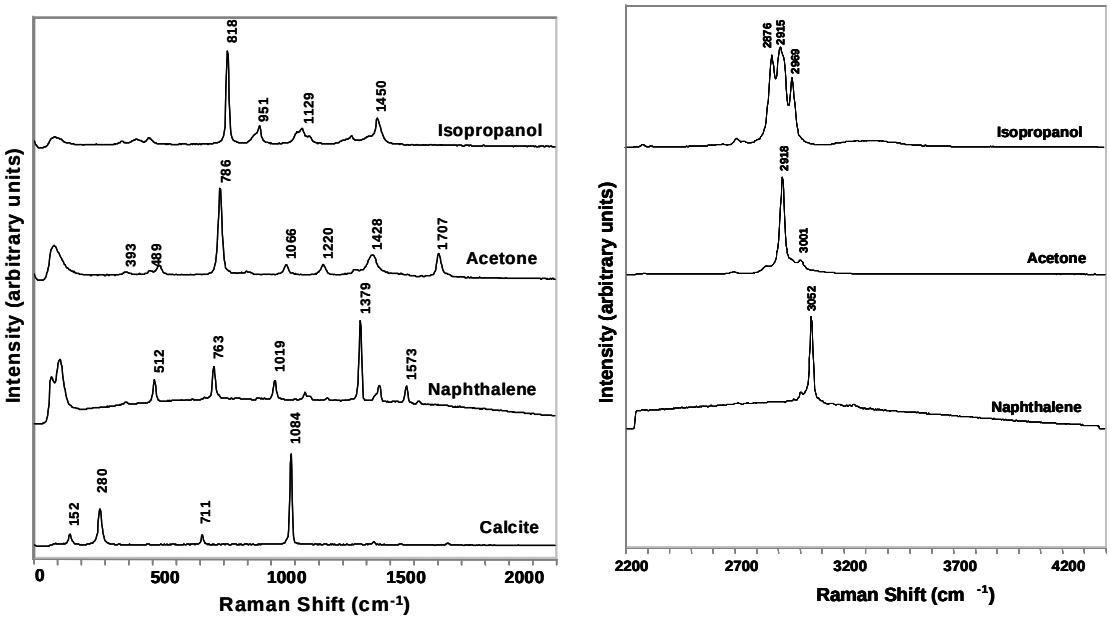

(a) (b)

Figure 2. Raman spectra of isopropanol, acetone, naphthalene, and calcite in the (a) low frequency, and (b) high frequency shift regions

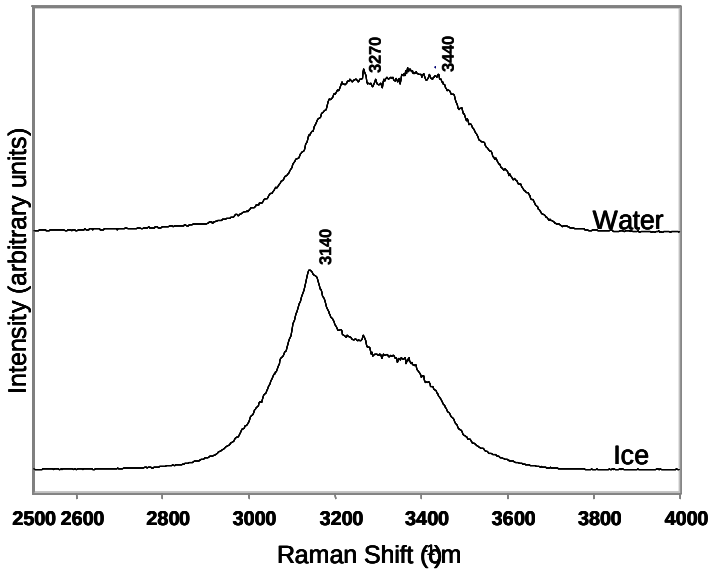

Figure 3. High frequency Raman spectra of liquid water and ice.

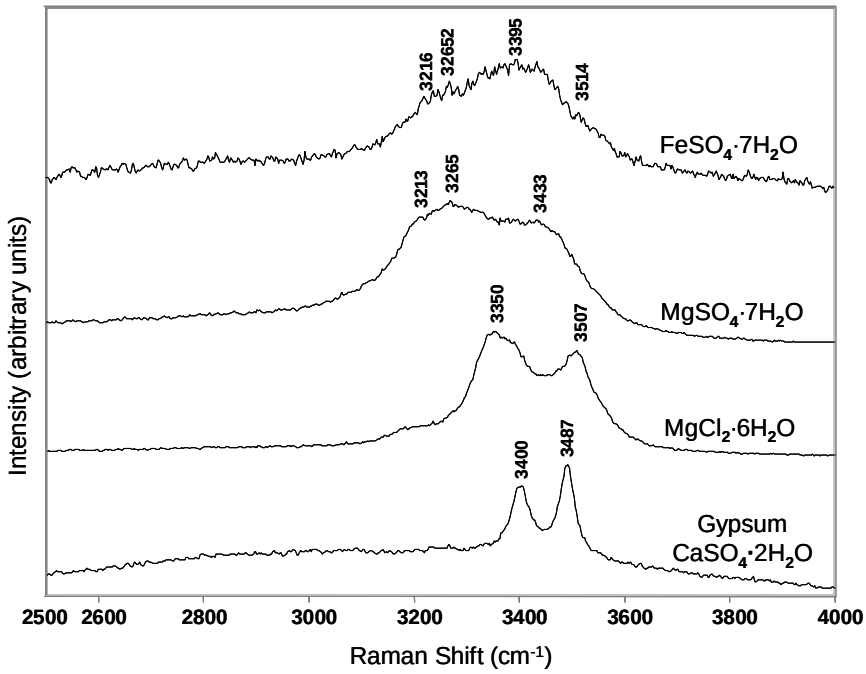

Figure 4. High frequency Raman spectra of hydrous minerals, $FeSO_4 \cdot 7H_2O$, $MgSO_4 \cdot 7H_20$, $MgCl_4 \cdot 6H_2O$, and gypsum.

5. CONCLUSION

A Raman spectroscopy system was demonstrated, having the ability to remotely measure the spectra of minerals, water, ice, and hydrous minerals, in light on condition. High quality spectra with very low background noise and without room-light spectral lines were produced with an integration time of 10 seconds by gating the detector. Moreover, the notch filter integrated in the spectrograph effectively blocked the strong Rayleigh-scattered photons. The calibration method using the spectral lines of a Neon source resulted in spectra which are accurate by about 2 cm^{-1}. The Raman spectra of standard samples, naphthalene, calcite, acetone, and isopropyl alcohol, verified the performance of the system. The spectra of ice and water clearly showed the Raman bands in the 3200 to 3500 cm^{-1} region, with ice having a distinguishing sharp band at 3140 cm^{-1}. Furthermore, the Raman bands due to the stretching modes of water molecules in hydrous minerals in the range 3200-3500 cm^{-1} are clearly observed and the frequencies of O-H stretching bands reflect their bonding of water molecules in these minerals .

REFERENCES

1. A. Wang, L. A. Haskin, A. L. Lane, T. J. Wdowiak, S. W. Squyres, R. J. Wilson, L. E. Howland, K. S. Manatt, N. Raouf, and C. D. Smith, "Development of Mars microbeam Raman Spectrometer," *J. Geophys. Res.*, 108(E1), 5005 (2003).
2. S. K. Sharma, S. M. Angel, M. Ghosh, H. W. Hubble, P. G. Lucey, "Remote pulsed Raman spectroscopy system for mineral analysis on planetary surfaces to 66 Meters," *Applied Spectroscopy*, 56, pp. 699-704, 2002.
3. J. I. Lunine, In search of planets and life around other stars, Proc. National Acd. Sci. 96, 5353, (1999).
4. A. K. Misra, S. K. Sharma, C. H. Chio and P. G. Lucey, Detection of water and water bearing minerals from 10 m distance under bright condition using remote Raman system, *Lunar and Planetary Sci. Conference*, 37, abstract #2155 (2006).
5. I. R. Lewis, H. G. M. Edwards, Eds., "*Handbook of Raman Spectroscopy*," Marcel Dekker, Inc., New York, pp. 1-10, 2001.
6. J. R. Ferraro, K. Nakamoto, "*Introductory Raman Spectroscopy*," Academic Press, Inc., San Diego, CA, pp. 7-17, 1994.

7. N. B. Colthup, L. H. Daly, S. E. Wiberley, "*Introduction to Infrared and Raman Spectroscopy*," 3rd Edition, Academic Press, Inc., San Diego, pp. 1-75, 1990.
8. Kaiser Optical Systems, Inc., "Holographic Notch Filters," Raman Products Technical Note No. 1050, http://www.kosi.com/raman/resources/technotes/1050.pdf.
9. Kaiser Optical Systems, Inc., "HoloPlex Holographic Transmission Grating," Raman Products Technical Note No. 1201, http://www.kosi.com/raman/resources/technotes/1201.pdf.
10. Princeton Instruments, PI-MAX/PI-MAX2 System Manual, Version 5.B, p. 17, 2004.
11. NIST Standard Reference Database Website: http://webbook.nist.gov/chemistry.
12. W. F. Cole and C. J. Launcuki, Arefinement of crystal structure of gypsum $CaSO_4 \cdot 2H_2O$, Acta Cryst. B30, 921, 1974.
13. C. H. Chio, S. K. Sharma, and D. W. Muenow, Raman spectroscopic studies of gypsum between 33 and 374 K, *Amer. Mineral.*, **89**, 390, 2004.
14. P. A. Agron and W. R. Busing, Magnesium dichloride hexahydrate, $MgCl_2.6H_2O$, by neutron diffraction, *Acta Cryst.*, C41, 8-10, 1985.
15. C. H. Chio, Shiv K. Sharma, and David W. Muenow, The hydrates and deuterates of ferrous sulfate ($FeSO_4$): a Raman spectroscopic study, *J. Raman Spectrosc*. (in press), 2006.
16. W. H. Baur, On the crystal chemistry of salt hydrates. III. The determination of the crystal structure of $FeSO_4.7H_2O$ (melanterite). *Acta Cryst.*, 17**,** 1167, 1964.
17. T .Kellersohn, R.G. Delaplane and I. Olovsson, Disorder of a trigonally planar coordinated water molecule in cobalt sulfate heptahydrate, $CoSO_4.7D_2O$ (Bieberite), *Z. Naturforsch.*, B 46, 1635, 1991.